Available online at www.sciencedirect.com
SCIENCE DIRECT®
International Journal of Non-Linear Mechanics 40 (2005) 795–805
INTERNATIONAL JOURNAL OF NON-LINEAR MECHANICS
www.elsevier.com/locate/nlm

Secondary buckling and tertiary states of a beam on a non-linear elastic foundation

Yin Zhang, Kevin D. Murphy*

Department of Mechanical Engineering, University of Connecticut, Storrs, CT 06268-3139, USA

Received 5 June 2003; received in revised form 10 February 2004; accepted 2 April 2004

Abstract

An axially compressed beam resting on a non-linear foundation undergoes a loss of stability (buckling) via a supercritical pitchfork bifurcation. In the post-buckled regime, it has been shown that under certain circumstances the system may experience a secondary bifurcation. This second bifurcation destablizes the primary buckling mode and the system "jumps" to a higher mode; for this reason, this phenomenon is often referred to as *mode jumping*. This work investigates two new aspects related to the problem of mode jumping. First, a three mode analysis is conducted. This analysis shows the usual primary and secondary buckling events. But it also shows stable solutions involving the third mode. However, for the cases studied here, there is no natural loading path that leads to this solution branch, i.e. only a contrived loading history would result in this solution. Second, the effect of an initial geometric imperfection is considered. This breaks the symmetry of the system and significantly complicates the bifurcation diagram.

Keywords: Secondary buckling; Tertiary solutions; Elastic foundation

1. Introduction

Directly following a buckling event, structures with a hardening non-linearity experience a dramatic rise in stiffness with increased axial load. Oftentimes, this increased stiffness far surpasses the pre-buckled stiffness, rendering the system even more stable than before. However, under very special circumstances, this post-buckled stiffness can again plummet with increased axial load and a secondary bifurcation occurs. First identified by Stein [1], this phenomenon causes the primary buckling mode to lose stability and the system "jumps" to a higher mode. Hence, this event is often referred to as *secondary buckling* or *mode jumping*.

To clarify what happens, consider the axially compressed beam resting on a non-linear elastic foundation, shown in Fig. 1a. The lateral displacement of the beam is traditionally comprised of its first two modes: $w(x) = Q_1 \sin(\pi x/L) + Q_2 \sin(2\pi x/L)$. Fig. 1b shows a schematic of the modal response as the axial load is gradually increased. Solid (dashed) lines are stable (unstable) equilibrium branches. At P_{cr}^1, the system buckles into the first mode. As the load is increased through P_{cr}^2, nothing unusual happens; the system remains buckled in the first mode and there is no contribution from the second mode. As the system is loaded to P_{cr}^{mj}, the first mode equilibrium solution loses sta-

* Corresponding author.

0020-7462/$ - see front matter © 2004 Published by Elsevier Ltd.
doi:10.1016/j.ijnonlinmec.2004.04.004

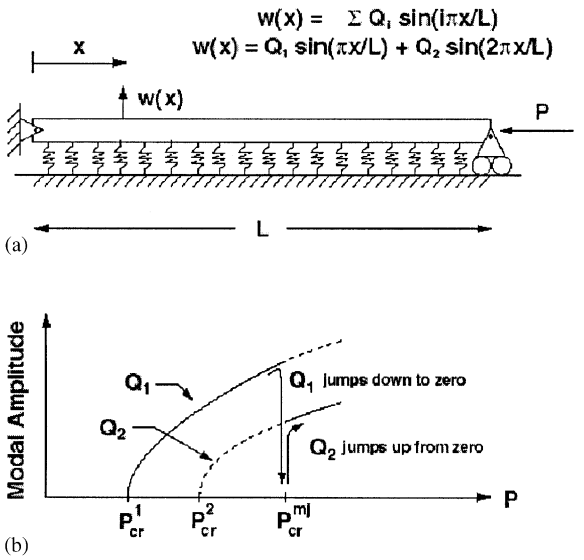

Fig. 1. (a) A schematic of the model system, (b) a schematic of typical mode jumping behavior.

bility and Q_1 drops to zero. Simultaneously, Q_2 jumps to a finite value. Beyond P_{cr}^{mj} the response depends on the specifics of the system under consideration. These different response scenarios are outlined by Supple [2]. Regarding this equilibrium diagram, two points should be made. First, in order to promote mode jumping early in the post-buckling regime, the buckling loads of the interacting modes are forced close together; this may be accomplished by a judicious choice in the beam length (or any other appropriate parameter). Second, on increasing the control parameter, mode jumping will only occur from a lower mode to a higher mode. So, for the case that $P_{cr}^2 < P_{cr}^1$ (a long beam) the system will not mode jump from the second mode to the first. Of course, for the scenario presented in the schematic, *reverse* mode jumping may also occur; the system may jump down (from the second mode to the first) as the control parameter is decreased.

Because of its detrimental influence in the post-buckled regime, mode jumping has received a good deal of attention since this phenomenon was first demonstrated in plate buckling [1]. As previously mentioned, Supple [2] described the different equilibrium branches that can emerge after mode jumping. This work was extended to look at evolving buckling patterns [3–5]. Others have examined the influence of various boundary conditions [6–8], lateral loads [9], and biaxially loading [10] on this phenomenon. More recently, Arnold tongues have been used to predict secondary buckling and to develop safety envelopes, within which secondary buckling cannot occur [8,11].

In the present paper, a third mode is incorporated into the structural model and mode jumping is reexamined. Specifically, the model consists of a linear elastic beam resting on a cubic non-linear foundation: $F_f = k_1(w_0 + w) + k_2(w_0 + w)^3$. The model also includes a small initial geometric imperfection (w_0), which breaks the symmetry of the system [2]. A three mode Galerkin discretization is used to arrive at a set of algebraic equilibrium equations, which are solved numerically using root solving and a pseudo-arclength method [12]. The results of the three mode system show that, in the absence of an imperfection, the primary and secondary bifurcations occur very much as they did when only two modes were retained. After the secondary bifurcation, the new stable branch is made up of only the second mode but the (now) unstable first mode branch couples with the third mode. As the axial load is increased further the stable second mode branch remains stable. However, another stable branch appears. This consists of just the third mode and is attainable only through an un-natural loading history, i.e. the system has to be forced to that solution. As a result, it is concluded that a two mode analysis is satisfactory for predicting behavior prior to mode jumping. But after the secondary bifurcation, alternate solution paths exist and should be considered.

2. Model development and solution techniques

2.1. Equations of equilibrium

The model system is shown in Fig. 1a. It consists of a linear elastic beam resting on a cubicly non-linear foundation. It is also subject to an axial compressive load P. To obtain the equilibrium equations the principle of virtual work is used. To accomplish this, expressions for the bending energy and the external work must be developed. The bending energy for a beam is

$$U_b = \frac{EI}{2}\int_0^L w_{,xx}{}^2\,dx, \tag{1}$$

where EI is the bending stiffness of the beam, w is the lateral deflection, and $\bullet_{,x} \equiv d\bullet/\mathrm{d}x$. Additional strain energy is stored in the foundation. For a foundation stiffness of $K = k_1 + k_2(w_0 + w)^2$, the force in the foundation is

$$F = [k_1 + k_2(w_0 + w)^2](w_0 + w). \tag{2}$$

And the potential energy stored by the foundation is

$$U_\mathrm{f} = \int_0^L \int_0^w F \,\mathrm{d}w \,\mathrm{d}x = \int_0^L \int_0^w [k_1 + k_2(w_0 + w)^2](w_0 + w) \,\mathrm{d}w \,\mathrm{d}x. \tag{3}$$

Work is done by the axial load P. It is expressed as

$$W = \frac{P}{2} \int_0^L (w_{,x} + w_{0,x})^2 \,\mathrm{d}x. \tag{4}$$

The Principle of Virtual Work asserts that $\delta(U_\mathrm{b} + U_\mathrm{f} - W) = 0$. Taking the necessary variations and integrating by parts leads to the following equilibrium equation:

$$EIw_{,xxxx} + P(w_{,xx} + w_{0,xx}) + (k_1 + 3k_2w_0^2)w + 3k_2w_0w^2 + k_2w^3 + (k_1w_0 + k_2w_0^3) = 0. \tag{5}$$

As shown in Fig. 1a, the boundaries are assumed to be pinned such that the boundary conditions are

$$w(0) = 0, \quad w_{,xx}(0) = 0, \quad w(L) = 0, \quad w_{,xx}(L) = 0. \tag{6}$$

It should be pointed out that if $k_1 = k_2 = 0$, Eq. (5) reverts to the standard linear imperfect beam model. Also, if the imperfection is eliminated ($w_0 = 0$), the non-linear equations studied in Ref. [7] are recovered.

Eq. (5) may be simplified by introducing the following non-dimensional quantities: $\xi = x/L$ and $W = w/L$. The result is

$$W_{,\xi\xi\xi\xi} + \beta_1 W_{,\xi\xi} + \beta_2 W + \beta_3 W^2 + \beta_4 W^3 + \beta_5 = 0, \tag{7}$$

where the coefficients to this equation are

$$\beta_1 = \frac{PL^2}{EI}, \quad \beta_2(\xi) = \frac{k_1 + 3k_2w_0^2}{EI} L^4, \quad \beta_3(\xi) = \frac{3k_2w_0}{EI} L^5, \quad \beta_4 = \frac{k_2}{EI} L^6, \quad \beta_5(\xi) = \left(\frac{k_1w_0 + k_2w_0^3}{EI} + \frac{PL^2}{EI} w_{0,\xi\xi} \right) L^3. \tag{8}$$

Obviously, β_2, β_3 and β_5 are functions of ξ because the initial imperfection is a function of ξ: $w_0 = w_0(\xi)$.

Eq. (7) is reduced to set of algebraic equations via Galerkin's method. A three term solution of the form

$$w = a_1 \sin(\pi\xi) + a_2 \sin(2\pi\xi) + a_3 \sin(3\pi\xi) \tag{9}$$

is assumed. This series is substituted into the equilibrium equation and Galerkin's method is carried out. This leaves three non-linear, algebraic equations in the unknown modal amplitudes a_1, a_2, and a_3; these are presented in the appendix. The numerical techniques used to solve these equations are outlined in the next section.

2.2. Numerical solutions techniques

The objective here is to obtain solutions to the discretized equilibrium equations as a function of the applied axial load. For an example, see the schematic result in Fig. 1b. For the majority of the simulations carried out in this work, the three non-linear equilibrium equations are solved numerically using a multidimensional Newton–Raphson routine. This technique is generally reliable but does encounter difficulties if the solution branch doubles back on itself, i.e. if the solution branch has a point of vertical tangency. In this case, the Newton–Raphson technique will jump off to a remote solution, rather than continuing on the present branch. To circumvent this problem, the tangent was constantly monitored. If the slope of the tangent exceeded a preset value, Newton–Raphson was abandoned and a pseudo-arclength (path-grabbing) method took over. This technique is outlined below but the interested reader is encouraged to read the more detailed description provided in Ref. [12].

The three equilibrium equations consist of three unknown modal amplitudes $\mathbf{a} = \{a_1, a_2, a_3\}$ and one control parameter P that is being varied. In the Newton–Raphson approach, P is gradually incremented; for each new P, a new solution vector $\mathbf{a}$ is found. The pseudo-arclength method still uses an incremental approach to solving the problem. But the problem is restated, such that the load P assumed to be an unknown.

Hence, the solution vector will consist of four quantities $\mathbf{a}' = \{P, a_1, a_2, a_3\}$ and, hence, another equation is required. This fourth equation is generated by requiring that the $(j+1)$th solution vector in the iterative scheme is not "too far" from the previous two solutions (the jth and $(j-1)$th). This can be expressed mathematically using quantities that resemble an L^2 norm:

$$\sum_{i=1}^{3} (a_i^{j+1} - a_i^j)(a_i^j - a_i^{j-1}) + (P^{j+1} - P^j)(P^j - P^{j-1}) = \sum_{i=1}^{3} (a_i^j - a_i^{j-1})^2 + (P^j - P^{j-1})^2. \quad (10)$$

By requiring sequential solutions to be *close by* in the 4-D vector space, this technique assures that the solution does not jump off to a remote solution.

2.3. Stability of equilibria

The local stability of an equilibrium solution (found using the techniques discussed in Section 2.2) may be ascertained in a number of ways. One common approach is to examine the curvature (i.e., the second derivatives) of the potential function [13]. Alternately, the stability may be studied by applying a small perturbation and observing the free response. The latter approach is taken here and necessitates adding an inertia term to Eq. (7). Specifically, the inertia term is $W_{,\tau\tau}$, where τ is a non-dimensional time and the mass has been absorbed into the non-dimensionalization. A perturbed solution of the form

$$W = W_{\text{eq}} + \hat{W} \quad (11)$$

is substituted into the governing dynamic equation (Eq. (7) + $W_{,\tau\tau}$), where $\hat{W}$ is a small oscillation superimposed on the equilibrium solution W_{eq}. Nonlinear terms in $\hat{W}$ are discarded and, given the equilibrium equation (Eq. (7)), the result is

$$\hat{W}_{,\tau\tau} + \hat{W}_{,\xi\xi\xi\xi} + \beta_1 \hat{W}_{,\xi\xi} + \beta_2 \hat{W} + 2\beta_3 W_{\text{eq}} \hat{W} + 3\beta_4 W_{\text{eq}}^2 \hat{W} = 0. \quad (12)$$

This equation is discretized using the expansion in Eq. (9) and Galerkin's method. Assuming a solution of the form $\hat{\mathbf{a}} = \hat{\mathbf{A}} e^{\lambda t}$, leads to an eigenvalue problem. These eigenvalues indicate the asymptotic stability of the particular equilibrium solution, $\mathbf{a}_{\text{eq}}$.

3. Results

3.1. The symmetric case

To consider initial buckling, the initial imperfection is removed ($w_0 = 0$) and the linearized version of Eq. (7) is used. From a stability analysis of this equation, the buckling load for each mode is given by

$$p_m = \frac{\pi^2 EI}{L^2}\left(m^2 + \frac{k_1 L^4}{m^2 \pi^4 EI}\right), \quad (13)$$

where m is the mode number. To demonstrate the general behavior of the system, the following parameters are used: $EI = k_1 = k_2 = 1$. Under these circumstances, Fig. 2 shows the critical load is as a function of the beam length. For the specific case of $L = 4.3$, the beam initially buckles in its first mode at a load of $P = 2.42$, as indicated by the circle; but it is close to the transition length of $L = 4.45$, which strongly promotes early mode jumping [2].

Before continuing, it should be noted that the structural response actually lives in a four dimensional space, made up of the control parameter and the three modal amplitudes (P, a_1, a_2, a_3). Obviously, we cannot present the response in the complete space (though a two mode analysis can be, see Ref. [14]). Instead, all of the amplitudes are superimposed on one common y-axis; however, it is useful to keep in mind that the expansion functions (mode shapes) are orthogonal and, hence, their amplitudes exist on mutually orthogonal axes.

Focusing on the mildly post-buckled regime, Fig. 3 shows the modal equilibria (3a) and the stability eigenvalues (3b) as a function of the axial compressive load, P. At low loads, the beam remains flat until it reaches point A; in the modal state space, this corresponds to $(P, a_1, a_2, a_3) = (2.42, 0, 0, 0)$. At a slightly larger load, the system has buckled into its first mode and the solution vector is $(P, a_1, 0, 0)$. This form of the solution vector continues with increasing P until point B. Here, this solution path loses stability and the system experiences standard *mode jumping*; the new stable solution has the form $(P, 0, a_2, 0)$. If the load is reduced, the system demonstrates hysteresis and the *reverse jump* occurs at a lower compres-

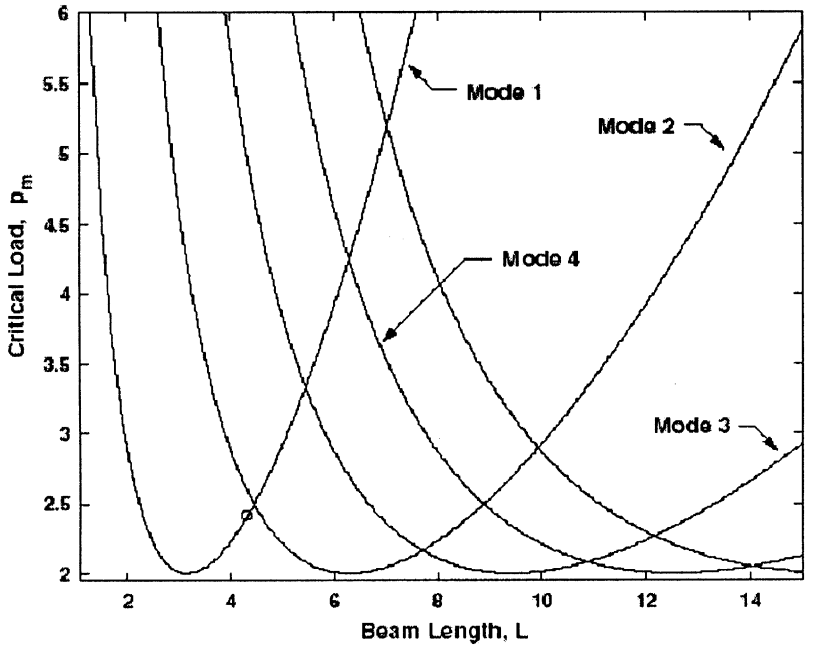

Fig. 2. Initial buckling loads for the system as determined by Eq. (13).

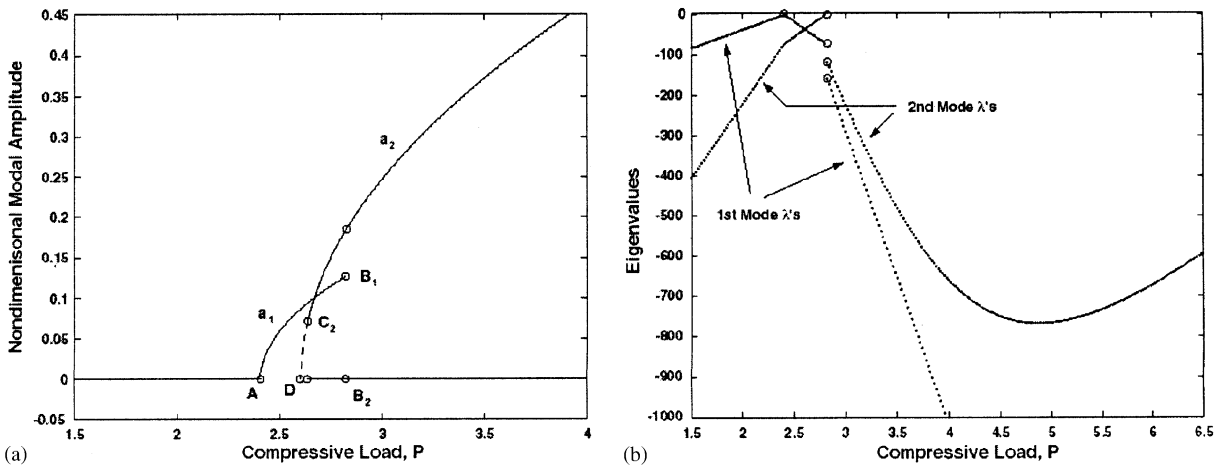

Fig. 3. (a) Equilibrium solutions for the symmetric, low-load case, (b) the associated stability eigenvalues for increasing load only.

sive load, i.e. at point C the stable solution switches from $(2.637, 0, 0.071, 0)$ to $(2.637, 0.0948, 0, 0)$. If P is reduced further, the unstable second mode solution will finally reach $(2.60, 0, a_2 \to 0, 0)$, which is the buckling point for the second mode. The stability of these solutions is confirmed by Fig. 3b. However, for the sake of clarity, only the stable solutions for the increasing load case have been shown in 3b. As the load is increased from zero, the eigenvalues transition smoothly up to initial buckling, where the first mode eigenvalue reaches zero. At this buckling point, the eigenvalue loci cusps as the eigenvalues are then cal-

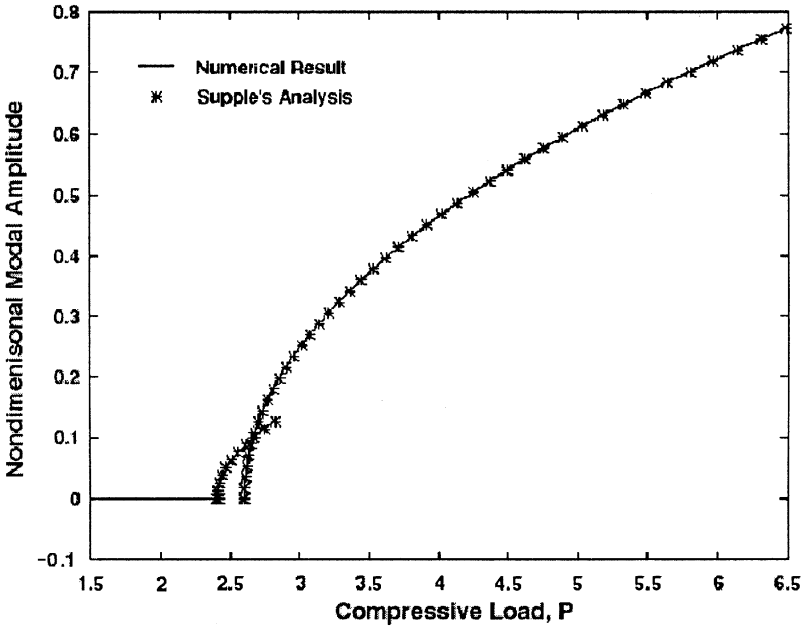

Fig. 4. Comparison of numerical results with Supple's (analytical) two mode results for the natural loading path.

culated about the newly stabilized, non-zero solution. As the load is increased still further, the system mode jumps. At this point, the second mode eigenvalue reaches zero and both eigenvalues discontinuously snap back to a stable (negative) value. It should also be noted that the numerical results compare well to Supple's analytical solutions in this low load regime for both increasing and decreasing load, as is shown in Fig. 4.

The aforementioned results capture the *initial* post-buckling behavior of the system and are consistent with those described previously by Everall and Hunt [7]. But now, let's focus on increasing the load beyond the initially post-buckled range. If the stable solution path is followed unperturbed (i.e., along $(P, 0, a_2, 0)$), nothing surprising happens. The second mode solution continues to grow, while a_1 and a_3 remain zero. However, if the unstable branch is followed (conceptually that is, not physically) a very different scenario ensues, see Fig. 5. After the mode jumping instability is encountered, the mode one (only) solution becomes unstable. The new unstable solution is a coupled solution of the form: $(P, a_1, 0, a_3)$. This behavior is shown in Fig. 5a (with 5b showing the stability). With increased load, these coupled amplitudes grow until point E, which corresponds to $(5.579, 0.344, 0, 0.184)$. At E, these unstable branches encounter a saddle node bifurcation and the system jumps to a stable equilibrium consisting of only the third mode: $(P, 0, 0, a_3)$. Because this *tertiary state* is the result of an instability from an unstable branch and has nothing to do with the previously existing stable solution, $(p, 0, a_2, 0)$, this solution branch is not naturally accessible. In other words, for this particular beam ($L = 4.3$), there is no natural loading history that can lead to this solution branch. Instead, an appropriate perturbation would have to be applied from the stable a_2 solution (for $P > P_E$) to arrive at the stable a_3 solution.

A more complete, albeit cluttered, equilibrium diagram for the symmetric system is shown in Fig. 6. This diagram more clearly demonstrates the coexisting stable solutions at higher compressive loads. It also shows more details about the saddle node bifurcation that occurs at point E, which causes the system to jump to the tertiary state. Using the continuation method, the unstable $(P, a_1, 0, a_3)$ solution is followed through the saddle node bifurcation

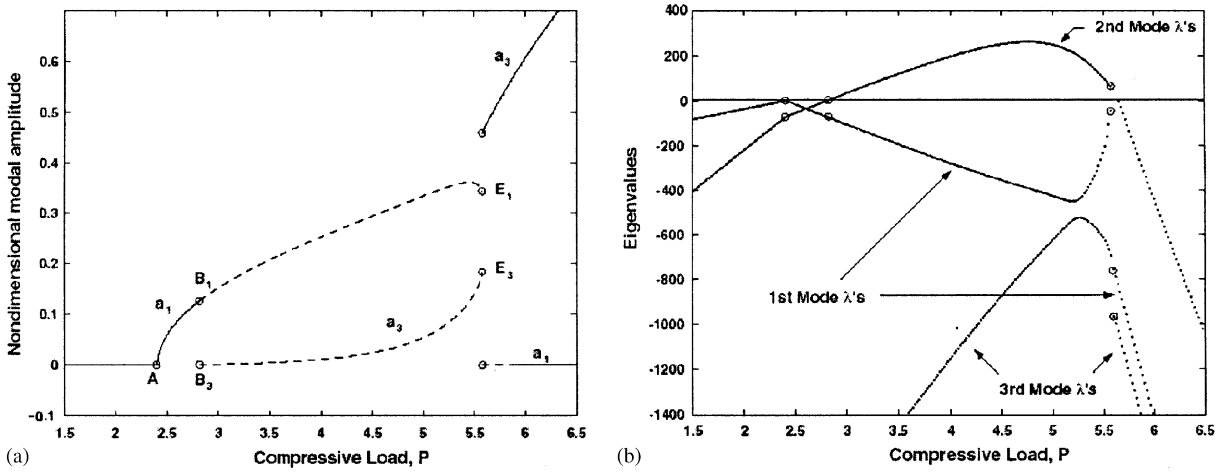

Fig. 5. (a) Equilibrium solutions for higher loads, showing tertiary states, (b) the associated stability eigenvalues.

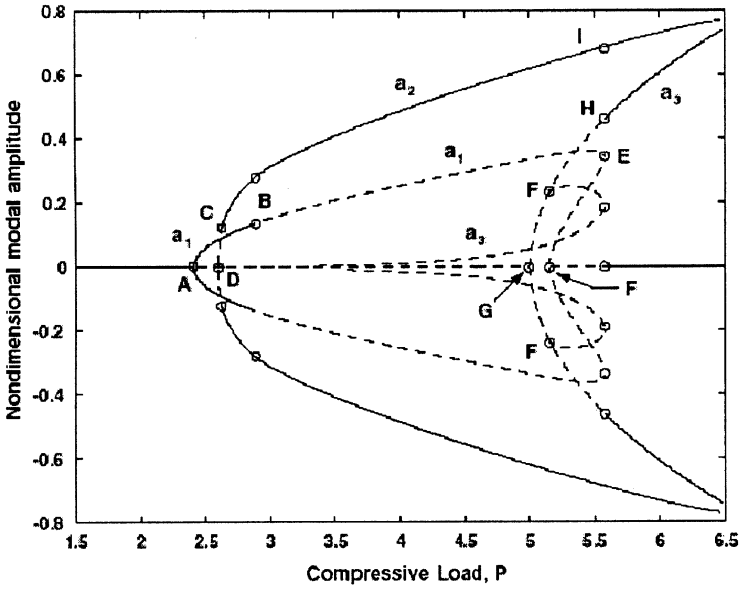

Fig. 6. The complete equilibrium diagram for the symmetric case.

at E and it is clear that at the vertical tangency there is no exchange of stability; it remains unstable. This coupled solution loops back on itself and continues until it experiences a pitchfork bifurcation at point F.

It is potentially instructive to see how these bifurcation amplitudes change under the influence of a control parameter, such as the beam length. This behavior is shown in Fig. 7. The lower two curves show the amplitudes at which the mode jumping occurs. The upper two curves show the amplitudes of the second and third mode at the appearance of the tertiary state (labeled point H and I in the Fig. 6). For a beam length of $L = 4.3$, which corresponds to the results of Figs. 3–6, the amplitudes are marked with circles. As

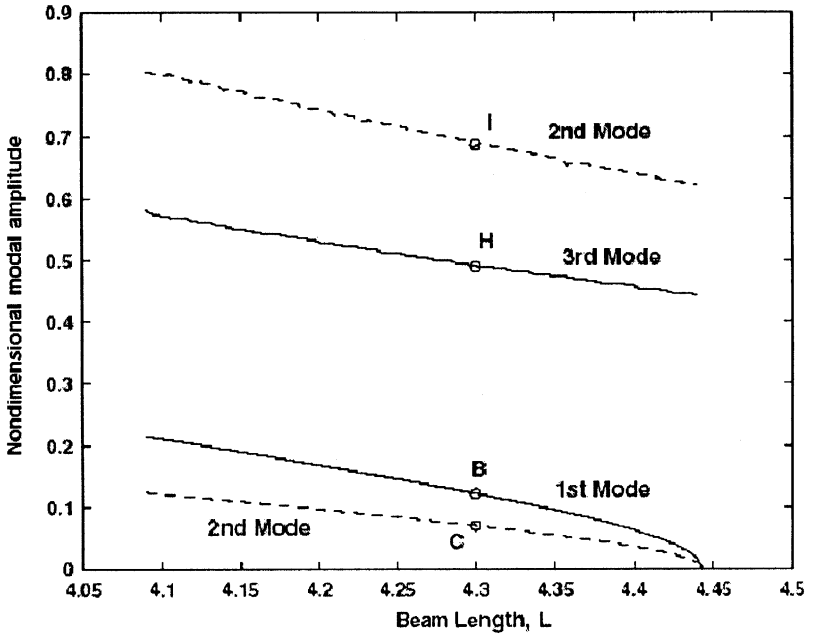

Fig. 7. A parameter study showing the influence of the beam length on the amplitudes corresponding to mode jumping (B and C) and the appearance of the tertiary state (H and I).

the beam length grows, the system approaches a double eigenvalue (see Fig. 2). In the process, the mode jump occurs at smaller and smaller amplitudes. Ultimately, as the length reaches $L = 4.45$, the eigenvalues coincide. Here the mode jumping amplitudes have shrunk to zero and the system begins to buckle in the second mode rather than the first; this precludes the possibility of mode jumping between the first and second mode. Furthermore, since the next double eigenvalue is far away, mode jumping is not likely to occur between the second and third mode. Likewise, the tertiary state has disappeared. Note that Fig. 7 contains roughly the same information that is available from an Arnold tongue plot [7]. However, that approach implicitly varies a parameter (the beam length) and does not provide information about jumps to tertiary states.

3.2. The asymmetric case

The asymmetric case corresponds to a non-zero value for w_0. Throughout this study, the imperfection is assumed to be in the first mode: $w_0(\xi) = 0.01\sin(\pi\xi)$. The equilibrium diagram corresponding to the natural loading path is shown in Fig. 8. In the low load regime, there is no buckling event. Instead, the first mode deflection grows steadily from the imperfection shape and is always coupled to the third mode, though the third mode contribution is extremely small. This behavior persists until this branch loses stability at point A, $(3.46, 0.251, 0, 0.008)$, and the system mode jumps. Unlike the symmetric case, where the stable solution after the mode jump was purely in the second mode, this new solution is a coupled mode one and mode two solution: $(P, a_1, a_2, 0)$. As the load is increased, the first mode contribution diminishes and the solution is dominated by the second mode. When unloaded, this solution branch again shows hysteresis. But the hysteresis involves both the first and second mode.

At high compressive loads, the system becomes somewhat more complex than its symmetric counterpart. As mentioned before, at A, the coupled mode one-mode three solution loses stability. This unstable behavior persists until point C $(5.459, 0.396, 0, 0.12)$, at which time the solution is briefly re-stabilized. As P is increased further, a saddle node bifurca-

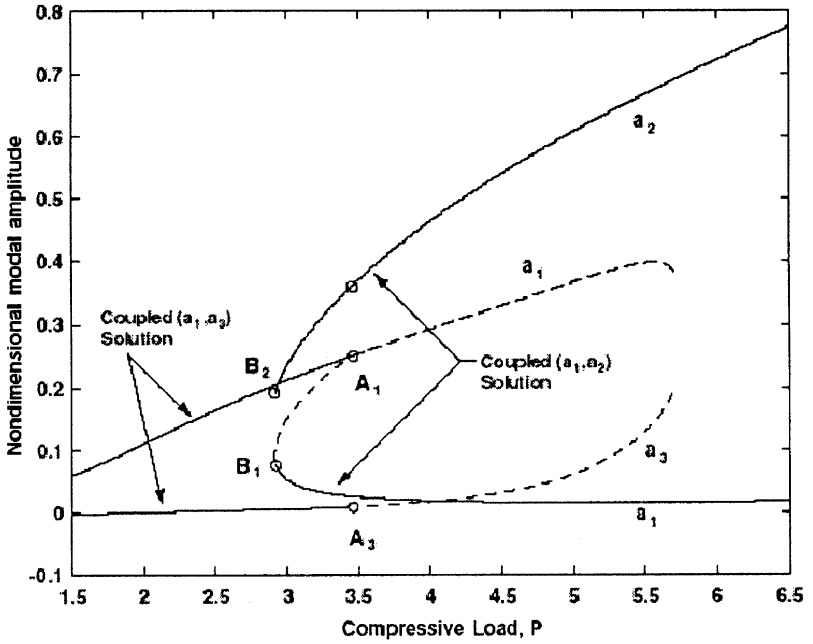

Fig. 8. Equilibrium solutions for the asymmetric, low-load case.

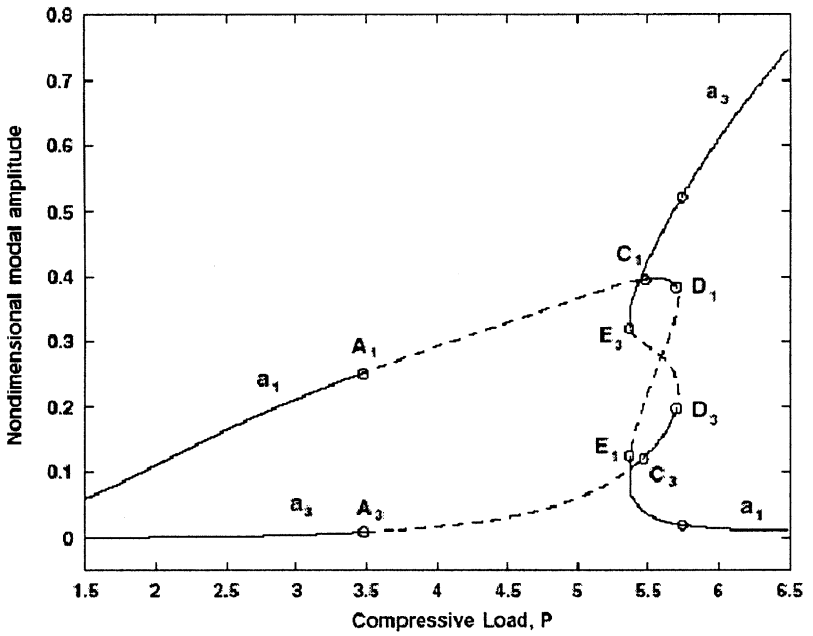

Fig. 9. Equilibrium solutions for the asymmetric case at higher loads, showing tertiary states.

tion is encountered at D $(5.74, 0.384, 0, 0.197)$ and the system jumps to the new (tertiary) solution $(5.74, 0.002, 0, 0.522)$. When unloaded, the solution is hysteretic and the stable tertiary solution loses stability at a saddle node bifurcation at E. As before, neither of these coupled mode 1–mode 3 solutions are realizable from the natural loading path (Fig. 9).

4. Conclusions

In this work, the secondary bifurcations and tertiary states of a beam resting on a non-linear elastic foundation have been investigated using a three mode approach. In addition, both the symmetric and asymmetric (geometrically imperfect) cases have been considered. For the symmetric case at low compressive loads, the system demonstrates the typical mode jumping from the first mode to the second mode, as well as hysteresis. At higher compressive loads another stable solution exists, which consists of the third mode only. However, for the beam under consideration ($L = 4.3$) there is no jump from the stable second mode solution to this stable third mode solution. A jump may occur (mathematically) from an unstable, coupled first and third mode solution. But a more physically realizable path is through a contrived loading history, i.e. pushing the system into this stable third mode solution from the stable second mode branch. It is interesting to note that a natural loading path may be created by pinning the left end and enforcing a *symmetric section condition*. This eliminates all unsymmetric behavior, thereby stabilizing the combined first and third mode solution and permitting the jump to the stable third mode (only) solution. Again, this is difficult to accomplish physically but is readily achieved mathematically.

The asymmetric case also demonstrates mode jumping at low compressive loads. However, at the higher compressive loads, there are actually three stable solutions. The first is the coupled mode 1–mode 2 solution, but this is dominated by the second mode. This arises from the natural loading path of the system. There are also two coupled mode 1–mode 3 solutions. One of these solutions ($a_1 > a_3$) is stable over a very small load level, whereas the other ($a_3 > a_1$) is stable over a much broader range of loads. As with the symmetric case, only a contrived loading history will lead to these solutions.

The upshot of this work is that at low loads, a simple two mode analysis will capture the essence of the behavior. However, at higher compressive loads, this system may demonstrate multiple stable equilibria containing higher modes. But, for the cases considered, these higher modal equilibria occur through non-natural loading paths.

Appendix.

The non-dimensional equilibrium equation, Eq. (7), may be discretized using Eq. (9) and Galerkin's method. Three non-linear algebraic equations for the three modal amplitudes result. These equations are: The a_1 equilibrium equation:

$$\left(\frac{\beta_2 - \pi^2\beta_1 + \pi^4}{2}\right) a_1 + \left(\frac{3\beta_4}{8}\right) a_1^3 + \left(\frac{3\beta_4}{4}\right) a_1 a_2^2 - \left(\frac{3\beta_4}{8}\right) a_1^2 a_3^2 + \left(\frac{3\beta_4}{8}\right) a_2^2 a_3 + \left(\frac{3\beta_4}{4}\right) a_1 a_3^2 + \left(\frac{4\beta_3}{3\pi}\right) a_1^2 + \left(\frac{16\beta_3}{15\pi}\right) a_2^2 - \left(\frac{8\beta_3}{15\pi}\right) a_1 a_3 + \left(\frac{36\beta_3}{35\pi}\right) a_3^2 + \left(\frac{2\beta_5}{\pi}\right) = 0.$$

The a_2 equilibrium equation:

$$\left(\frac{\beta_2 - 4\pi^2\beta_1 + 16\pi^4}{2}\right) a_2 + \left(\frac{3\beta_4}{4}\right) a_1^2 a_2 + \left(\frac{3\beta_4}{8}\right) a_2^3 + \left(\frac{3\beta_4}{4}\right) a_1 a_2 a_3 + \left(\frac{3\beta_4}{4}\right) a_2 a_3^2 + \left(\frac{32\beta_3}{15\pi}\right) a_1 a_2 + \left(\frac{32\beta_3}{21\pi}\right) a_2 a_3 = 0.$$

The a_3 equilibrium equation:

$$\left(\frac{\beta_2 - 9\beta_2\pi^2 + 81\pi^4}{2}\right) a_3 - \left(\frac{\beta_4}{8}\right) a_1^3 + \left(\frac{3\beta_4}{8}\right) a_1 a_2^2 + \left(\frac{3\beta_4}{4}\right) a_1^2 a_3 + \left(\frac{3\beta_4}{4}\right) a_2^2 a_3 + \left(\frac{3\beta_4}{8}\right) a_3^3$$

$$-\left(\frac{4\beta_3}{15\pi}\right)a_1^2+\left(\frac{16\beta_3}{21\pi}\right)a_2^2+\left(\frac{72\beta_3}{35\pi}\right)a_1a_3 +\left(\frac{4\beta_3}{9\pi}\right)a_3^2+\left(\frac{2\beta_5}{3\pi}\right)=0.$$

References

[1] M. Stein, Loads and deformations of buckled rectangular plates, NASA TR T-40, 1959.

[2] W.J. Supple, Coupled branching configurations in the elastic buckling of symmetric structural systems, Int. J. Mech. Sci. 9 (1967) 97–112.

[3] W.J. Supple, On the change in buckling pattern in elastic structures, Int. J. Mech. Sci. 10 (1968) 737–745.

[4] W.J. Supple, Initial post-buckling behavior of a class of elastic structural systems, Int. J. Nonlinear Mech. 4 (1969) 23–36.

[5] W.J. Supple, Changes of wave-form of plates in the post-buckling range, Int. J. Solids Struct. 6 (1970) 1243–1258.

[6] D.G. Schaeffer, M. Golubitsky, Boundary conditions and mode jumping in the buckling of rectangular plates, Commun. Math. Phys. 69 (1979) 209–236.

[7] P.R. Everall, G.W. Hunt, Quasi-periodic buckling of an elastic structures under the influence of changing boundary conditions, Proc. R. Soc. London, Ser. A 455 (1999) 3041–3051.

[8] P.R. Everall, G.W. Hunt, Mode jumping in the buckling of struts and plates: a comparative study, Int. J. Nonlinear Mech. 35 (2000) 1067–1079.

[9] H. Steinruck, H. Troger, R. Weiss, Mode jumping of imperfect, buckled, rectangular plates, Int. J. Numer. Math. 70 (1984) 515–524.

[10] R. Maaskant, J. Roorda, Mode jumping in biaxially compressed plates, Int. J. Solids Struct. 29 (1992) 1209–1219.

[11] P.R. Everall, G.W. Hunt, Arnold Tongue predictions of secondary buckling in thin elastic plates, J. Mech. Phys. Solids 47 (1999) 2187–2206.

[12] H.B. Keller, Lectures on Numerical Methods in Bifurcation Problems, Springer, Berlin, 1987.

[13] J.M.T. Thompson, G.W. Hunt, A General Theory of Elastic Stability, Wiley, New York, 1973.

[14] H. Suchy, H. Troger, R. Weiss, A numerical study of mode jumping, Z. Angew. Math. Mech. 65 (2) (1985) 71–78.